

The cross sections of fusion-evaporation reactions: the most promising route to superheavy elements beyond $Z=118$

Khuyagbaatar Jadambaa^{1,2,*}

¹Helmholtz Institute Mainz, 55099 Mainz, Germany

²GSI Helmholtzzentrum für Schwerionenforschung, 64291 Darmstadt, Germany

Abstract. The synthesis of superheavy elements beyond oganesson (Og), which has atomic number $Z = 118$, is currently one of the main topics in nuclear physics. An absence of sufficient amounts of target material with atomic numbers heavier than californium ($Z = 98$) forces the use of projectiles heavier than ^{48}Ca ($Z = 20$), which has been successfully used for the discoveries of elements with $Z = 114 - 118$ in complete fusion reactions. Experimental cross sections of ^{48}Ca with actinide targets behave very differently to “cold” and “hot” fusion-evaporation reactions, where doubly-magic lead and deformed actinides are used as targets, respectively. The known cross sections of these reactions have been analysed compared to calculated fission barriers. It has been suggested that observed discrepancies between the cross sections of ^{48}Ca -induced and other fusion-evaporation reactions originate from the shell structure of the compound nucleus, which lies in the island of the stability. Besides scarcely known data on other reactions involving heavier projectiles, the most promising projectile for the synthesis of the elements beyond Og seems to be ^{50}Ti . However, detailed studies of ^{50}Ti , ^{54}Cr , ^{58}Fe and ^{64}Ni -induced reactions are necessary to be performed in order to fully understand the complexities of superheavy element formation.

1 Introduction

The search for “hypothetical” nuclei from the island of stability, referred to as superheavy nuclei (SHN), which are predicted to be located at around proton number $Z = 114$ and neutron number $N = 184$ according to most theoretical calculations [1–3], is the one of the main goals of fundamental nuclear physics research. To date, isotopes of elements up to $Z = 118$ and $N = 177$ have already been discovered [4]. The heaviest elements ($Z = 114 - 118$) have been directly produced in ^{48}Ca -induced reactions with actinide targets, first at Dubna Gas-Filled Recoil Separator (DGFRS) at the Flerov Laboratory of Nuclear Reactions in Dubna, Russia. The findings of these works were confirmed world-wide by different laboratories using the same reactions [5–15]. Recently, four elements with $Z = 113, 115, 117$ and 118 have officially been named as nihonium (Nh), moscovium (Mc), tennessine (Ts) and oganesson (Og), respectively [16].

Presently, the synthesis of elements beyond Og is the hot topic in the research field, despite that the predicted magic $Z = 114$ has already been reached. However, an absence of sufficient amounts of target material with atomic numbers heavier than californium ($Z = 98$) currently prevents the use of ^{48}Ca for synthesis of elements beyond Og. The predicted magic $N = 184$ also remains out of reach due to limited access to both radioactive beams and appropriate target materials.

Of special interest is the element with $Z = 120$, wherein some theories predict a stronger shell closure compared to the “classical” magic $Z = 114$ i.e. a shift in the location of the center of the island of stability. Several attempts to synthesize the element with $Z = 120$ have already been carried out using $^{64}\text{Ni}+^{238}\text{U}$ [17], $^{58}\text{Fe}+^{244}\text{Pu}$ [18], $^{54}\text{Cr}+^{248}\text{Cm}$ [19], and $^{50}\text{Ti}+^{249}\text{Cf}$ [20] reactions. However, none of these studies reported observation of the element with $Z = 120$, despite reaching sensitivity levels that would be sufficient to detect at least one event from any of the known ^{48}Ca -induced reactions. This non-observation can firstly be due to entrance-channel effects [21], as the coulomb repulsion forces of these reactions are significantly greater than those for ^{48}Ca -induced reactions. Secondly, the survival probabilities of compound nuclei could also be smaller when compared with Og, according to most theoretical predictions [1–3]. Also, impacts of the double magicity ($Z = 20$ and $N = 28$) of ^{48}Ca on capture, fusion and survival probabilities are still not yet fully understood [22] despite its effect on the reaction Q -value.

However, knowledge of the effect of these two processes remains poor, not only for elements beyond Og but also for lighter ones. For the observation of a single atom of a superheavy element, experiments must often be performed for several days, weeks or months [4–15, 17–20, 23]. Therefore, choosing a suitable projectile-target combination and optimum beam energy for a reaction are of utmost importance to maximize the countable yield of heavy nuclei.

*e-mail: J.Khuyagbaatar@gsi.de

The cross sections of ^{48}Ca -induced fusion-evaporations reactions with actinide targets remain at the level of pbarns as a function of Z of the compound nucleus (Z_{CN}), as opposed to those of “cold”- and “hot”-fusion reactions (where doubly-magic lead and deformed actinides are used as targets, respectively), which decrease exponentially. It has already been suggested that such behaviour is associated with the survival probability of the compound nucleus [4].

In the present paper, a compilation of the known data on ER cross sections of the above mentioned reactions were performed and tested for a presence of any systematic trends. This would help to understand the discrepancy in the case of ^{48}Ca , and may also be useful for the selection of preferable projectile and target combinations leading to elements beyond Og.

2 The cross sections of the fusion-evaporation reactions

Since all of the SHN have been exclusively produced in fusion-evaporation reactions, their experimental cross sections may provide an important information on the preferable choice of projectile and target combinations for the synthesis of the as yet unknown SHN. The evaporation residue (ER) cross section of fusion reactions passing through a formation of compound nucleus (CN) is often described by the three-term expression,

$$\sigma_{ER}(E^*, J) = \sigma_{cap}(E, J)[1 - P_{QF}(E, J)]W_{CN}(E^*, J), \quad (1)$$

where σ_{cap} is the cross section characterizing the formation of the di-nuclear system (capture) at collision energy E , P_{QF} is the fraction of di-nuclear systems not evolving via formation of CN with a compact shape i.e. splitting into two fragments (quasi-fission), and W_{CN} is the survival probability of CN against fission through particle evaporation at the excitation energy of $E^* = E - Q$, where Q is the energy necessary for the fusion. Terms σ_{cap} and W_{CN} describe independent processes and have been studied substantially, both experimentally and theoretically.

A theoretical description of P_{QF} , or its complementary $P_{CN}=1-P_{QF}$, which characterizes the fusion probability, is not yet fully developed [24, 25]. The main problem is the dynamical evolution of the multidimensional di-nuclear system leading to equilibration in all possible degrees of freedom, which is still not describable despite developments in modern theory and computing. Therefore, P_{CN} is often extrapolated from the experimental observations of the nuclear reaction studies [26]. In the earlier studies, where mostly the light particles/ions were used as a projectile, the quasi-fission probability was shown to be negligible. With more massive ion beams with $Z > 20$ that gave access to superheavy elements, a reduction of P_{CN} has been observed due to quasi-fission. In reactions with strong coulomb repulsion forces between the collision partners ($Z_p Z_t > 1600$), the presence of quasi-fission was predicted [27]. As a result, σ_{ER} for fusion reactions leading to the formation of SHN drastically decreases as function of Z_{CN} or $Z_p Z_t$.

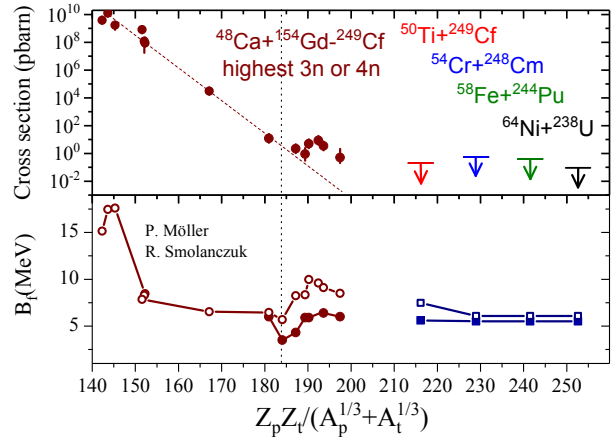


Figure 1. a) Compiled experimental ER cross sections of fusion-evaporation reactions with ^{208}Pb and ^{238}U targets, and ^{48}Ca projectiles [28–32]. Only maximum values of σ_{1n} and σ_{5n} are shown for ^{208}Pb and ^{238}U , respectively. Maximum values of either σ_{3n} or σ_{4n} from ^{48}Ca -induced reactions with deformed Gd-Cf targets are shown. Arrows mark upper limits. Dashed lines are drawn to guide an exponential descent. b) Theoretical $B_f - S_n$ calculated within the macro-microscopic FRDM approach are given [3, 37].

2.1 “Cold”, “hot” and ^{48}Ca -induced fusion reactions

Compiled ER cross sections of three types of fusion reactions are shown in Fig. 1 as a function of $Z_p Z_t / (A_p^{1/3} + A_t^{1/3})$ parameter which is equivalent to the Coulomb repulsion at contact between spherically shaped projectile and target nuclei. This or any other variables like effective entrance channel fissility are better for displaying the reaction entrance channel than Z_{CN} or $Z_p Z_t$. As representatives of “cold”, and “hot” fusion, the maxima cross sections of 1 and 5 neutron evaporation channels, σ_{1n} and σ_{5n} , of reactions with ^{208}Pb and ^{238}U targets, respectively, were compiled [28, 29, 32]. In the case of the ^{48}Ca -induced reactions, only maximum of σ_{3n} or σ_{4n} with deformed targets were selected to test for any systematic trend. In this case the well-known orientation effect of the collision will be accounted for [24, 33, 34].

In the statistical model, the survival probability of the excited nucleus has an exponential dependence on the fission barrier, B_f , and neutron separation energy, S_n and is often expressed as

$$W_{CN}(E^*) \sim \prod_i^x e^{[(B_f - S_n)/T]_i},$$

where T and x are the temperature and number of emitted neutrons from the CN. The latter depends on available E^* of the nucleus populated at each stage.

The fission probability of the highly-excited heavy nucleus strongly increases as function of E^* [35]. Thus, the survival probability of the initial CN which has highest possible E^* , against the fission (first-chance fission) is the most crucial process for residue formation [25, 36]. Accordingly, $B_f - S_n$ value of the initial CN can be applied for comparative analysis of W_{CN} . The calculated $B_f - S_n$

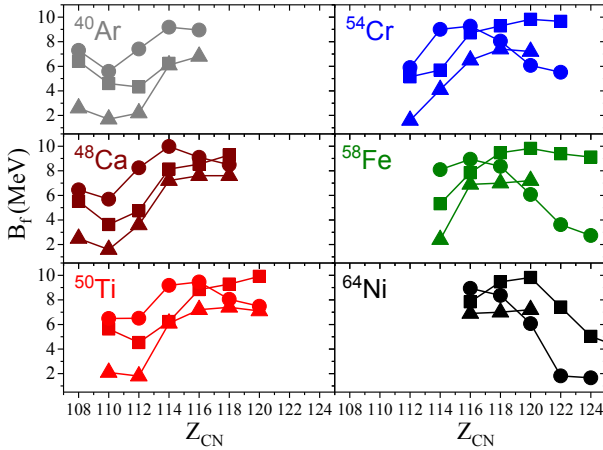


Figure 2. Calculated fission barriers of SHN, which can be formed as CN in ^{40}Ar , ^{48}Ca , ^{50}Ti , ^{54}Cr , ^{58}Fe and ^{64}Ni -induced reactions with available actinide targets, ^{226}Ra - ^{249}Cf . The results from FRDM [37], HBF(Sk*) [40] and ETFSI [41] calculations are given by dots, squares and triangles, respectively.

of the initial CN corresponding to each reaction are shown in Fig. 1b) as a representative for the W_{CN} . Both variables have been extracted from the same mass FRDM-calculations [3, 37] to exclude systematic uncertainties due to the theoretical approaches.

Firstly, all three types of reactions have a decreasing trend of their σ_{ER} as a function of the coulomb parameter i.e. Z_{CN} , except in the case of ^{48}Ca leading to elements heavier than Hs ($Z = 108$). The decreasing slope is steeper in ^{48}Ca -induced reactions compared to other two, which have a similar slopes. As mentioned above, the fusion-evaporation reaction is the output of three consecutive physical processes. Accordingly, observed trends might have different origins. In “hot” fusion reactions where the coulomb repulsion force is smaller i.e., $Z_p Z_t < 1600$, QF was believed to be negligibly small. However this criteria has been shown to be obsolete i.e. experimental evidence for the presence of QF in reactions with $Z_p Z_t < 1600$ has been observed [25, 38]. In “cold” fusion reactions where $Z_p Z_t > 1600$, it is well known that QF dominates over fusion [27]. In addition, compiled σ_{in} of this type of reaction have been observed at energies below the fusion barrier, where σ_{cap} steeply decreases. Trends of $B_f - S_n$ for these two types of reactions do not show a significant difference (within the chosen scale of vertical axis) and vary smoothly as function of Z_{CN} . Therefore, the decreasing σ_{ER} trend of “cold” fusion reactions could mostly be driven by entrance channel effects which can modify both capture cross sections and fusion probabilities.

In the case of ^{48}Ca , $B_f - S_n$ values follow a U-shape as function of Z_{CN} , and initially decrease with increasing Z_{CN} up to Ds ($Z = 110$). This may explain the observed steeper decrease of σ_{ER} compared to other two reactions. (i) After Ds, $B_f - S_n$ rises again as B_f falls under the influence of the shell closure originating from the island of stability, thus impacting on W_{CN} and increasing the σ_{ER} . Consequently,

σ_{ER} of SHN beyond Ds that are enhanced compared to the expected exponential descent could be due to W_{CN} [39].

To test the above-mentioned suggestion (i) initially proposed in Ref. [39], the results of other theoretical predictions of B_f are examined. Fission barriers calculated within three different theoretical models are shown in Fig. 2. The results of FRDM compared to two other theoretical models, both microscopic self-consistent calculations performed within the Hartree-Fock-Bogoliubov (HFB) approximation with the SkM* force [40] and Extended Thomas-Fermi plus Strutinsky Integral model (ETFSI) based on Skyrme SkSC4 functional [41], are shown.

Predicted fission barriers of CN formed in ^{40}Ar , ^{50}Ti , ^{54}Cr , ^{58}Fe and ^{64}Ni -induced reactions with ^{226}Ra - ^{249}Cf actinide targets are also shown in Fig. 2, in addition to those formed in ^{48}Ca -induced reactions.

Overall, they all predict the existence of the island of stability despite their quantitative discrepancies. However, a precise prediction of an absolute B_f is presently still not yet established for heaviest nuclei and results often differ from experimental ones by up to several MeV [42]. In spite of this, they all predict an increasing tendency of B_f after passing Ds in the ^{48}Ca cases, thus supporting the arguments made in point (i) discussed above. One interesting feature can be noted in the case of CN formed in the $^{40}\text{Ar} + ^{248}\text{Cm}$ reaction, where the calculations predict a similarly high B_f as for the $^{48}\text{Ca} + ^{244}\text{Pu}$ and/or $^{48}\text{Ca} + ^{242}\text{Pu}$ reactions where the σ_{ER} are known. One has to emphasize that it will be interesting to measure σ_{ER} of $^{40}\text{Ar} + ^{248}\text{Cm}$ in order to help to understand the differences in the reaction mechanism.

Obvious differences in between theories can be found in cases where reactions lead to elements beyond Og because they predict differing values of Z to be magic. For example, FRDM calculations predict a magic proton number at $Z = 114$, compared to $Z = 120$ in HFB(Sk*), as can be clearly seen in Fig. 2. If the latter prediction is correct, then one may expect to observe a more enhanced W_{CN} of CN with $Z = 120$ compared to Cn-Og, which may also increase the σ_{ER} . Thus, the synthesis of the element with $Z = 120$ and measuring its production cross section will help to solve persistent discrepancies in the theoretical models.

2.2 The reactions leading to formation of elements beyond 118

For the synthesis of the element with $Z = 120$, ^{48}Ca is can not presently be used, thus one needs to use a heavier projectiles like ^{50}Ti , ^{54}Cr , ^{58}Fe , ^{64}Ni etc.. The experimental cross-section sensitivities of four different reactions leading to formation of element $Z = 120$, $^{64}\text{Ni} + ^{238}\text{U}$ [17], $^{58}\text{Fe} + ^{244}\text{Pu}$ [18], $^{54}\text{Cr} + ^{248}\text{Cm}$ [19], and $^{50}\text{Ti} + ^{249}\text{Cf}$ [20], are shown in Fig. 3 together with ^{48}Ca results. Values of calculated $B_f - S_n$ for CN calculated within the FRDM framework are also shown. To make a consistent comparison of σ_{ER} to those discussed in the previous section, the known data (maximum of either σ_{3n} or σ_{4n} on ^{50}Ti , ^{54}Cr ,

^{58}Fe and ^{64}Ni -induced reactions with deformed Gd-Cf targets are compiled.

As seen from Fig. 3 data on these reactions are scarce. A decreasing trend can only be drawn in the case of ^{50}Ti , which falls off much steeper than for ^{48}Ca (cf. Fig. 3a). However, it is probably not a realistic case for extracting a slope as the ER from the $^{50}\text{Ti}+^{176}\text{Yb}$ is an extremely neutron-deficient isotope of U ($Z = 92$) [43], and thus W_{CN} may be strongly reduced.

This is also the case for the $^{48}\text{Ca}+^{181}\text{Ta}$ reaction (see Fig. 3a), where recently measured upper limit [44] is not following the extrapolated exponential. Therefore, one can assume a similar slope for all reactions including ^{48}Ca data, although these need to be measured. Extrapolated exponentials, fitted to the known data of the particular reaction and assuming the same slope as for ^{48}Ca , are shown in Fig 3a.

In all four reactions leading to $Z = 120$ formation discussed here ($^{64}\text{Ni}+^{238}\text{U}$, $^{58}\text{Fe}+^{244}\text{Pu}$, $^{54}\text{Cr}+^{248}\text{Cm}$, and $^{50}\text{Ti}+^{249}\text{Cf}$), one might expect a similar increase of W_{CN} due to shell effects originating from the island of stability as seen in ^{48}Ca -induced reactions (discussed in (i)). The CN is the same in all cases except for $^{50}\text{Ti}+^{249}\text{Cf}$, where the CN has three fewer neutrons, but the B_f values are similar. From the known ^{48}Ca cross sections, leading to the formation of Fl-Og, this gain in cross section via the W_{CN} enhancement can be estimated to be roughly two orders of magnitude higher than an exponential descent. One might then tentatively expect a similar gain in σ_{ER} with respect to an exponential extrapolated, to be observed in reactions leading to $Z = 120$.

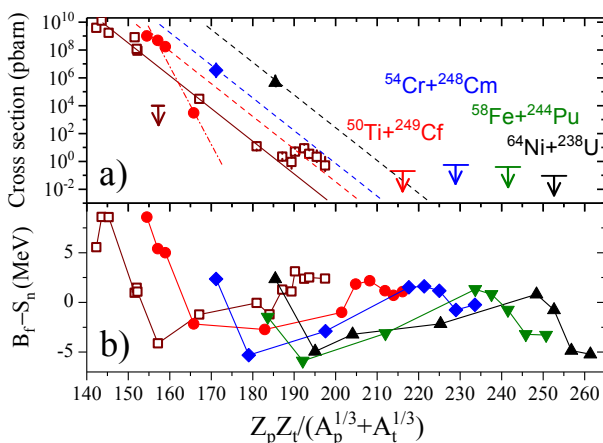


Figure 3. a) The compiled maximum of either σ_{3n} or σ_{4n} [28, 29, 32, 43, 45] and b) calculated CN's $B_f - S_n$ within the FRDM model [3, 37] are given for ^{48}Ca (open symbols), ^{50}Ti (dots), ^{54}Cr (rhombuses), ^{58}Fe (down-triangles) and ^{64}Ni (up-triangles) induced reactions with deformed Gd-Cf targets. a) Cross-section sensitivities are marked by arrows [17–20, 44]. Solid line is drawn to guide an exponential descent of σ_{ER} in ^{48}Ca -induced reactions up to formation of Hs and continued to higher Z_{CN} . Dashed-dotted line shows a trend of known σ_{ER} for ^{50}Ti -induced reactions. Dashed lines are the same as the solid one but shifted to fit known σ_{ER} of the particular reaction. See text for details

As the coulomb forces increase significantly when changing from ^{48}Ca to a heavier projectile, the extrapolated σ_{ER} decrease dramatically for a fixed Z_{CN} . Accordingly, reactions involving projectile and target combinations with the smallest coulomb forces are preferable for synthesizing element $Z = 120$. Although the resulting σ_{ER} estimate for the $^{50}\text{Ti}+^{249}\text{Cf}$ reaction of up to several fbarns (10^{-3} pbarns) is not very encouraging and is about two-three orders of magnitude smaller than those for ^{48}Ca -induced reactions, the true cross section could be quite different and therefore it is of great importance that the values be measured experimentally.

Note that the use of ^{50}Ti as a projectile also gives access to SHN with $Z = 114 - 118$, whereas the range of accessible SHN with heavier projectiles appears to be even more limited, within the current capabilities and level of understanding of the fusion-evaporation reaction.

3 Summary and outlook

The compiled ER cross sections of three different types of fusion-evaporation reaction were comparatively analysed relative to the calculated fission barriers (\sim survival probability) from three different theoretical models. All three types of reaction (namely "cold", "hot" and ^{48}Ca -induced) show a similar decreasing trend of the ER cross sections as functions of the proton numbers in the compound nucleus. The known discrepancy in ER cross sections of ^{48}Ca with actinide targets were suggested to occur due to an enhanced survival probability of compound nuclei originating from shell closures associated with the island of stability, shown independently by the different theoretical frameworks discussed here.

A similarly enhanced survival probability for reactions leading to $Z = 120$ may also be expected, providing an important testing ground for theories which, although they interpret the behaviour of ^{48}Ca +actinide results well, may not produce an accurate description for heavier systems. Experimental data on ER cross sections of reactions involving heavier projectiles and deformed targets, which are necessary for reaching $Z = 120$, are very scarce. Thus, more measurements must be made.

Based on the present analysis, the main differences in the ER cross section of reactions $^{64}\text{Ni}+^{238}\text{U}$, $^{58}\text{Fe}+^{244}\text{Pu}$, $^{54}\text{Cr}+^{248}\text{Cm}$, and $^{50}\text{Ti}+^{249}\text{Cf}$ leading to element with $Z = 120$ could be strongly due to their entrance channel effects. One can argue that the latter reaction with smallest $Z_p Z_t$ might be the most preferable for a making the superheavy element with $Z = 120$. For a final conclusion to be made on which reactions are preferable, further investigations of fusion and quasi-fission processes must be performed.

References

- [1] A. Sobiczewski et al., Phys. Lett. **22**, 500 (1966).
- [2] W.D. Myers and W.J. Swiatecki, Nucl. Phys. **81**, 1 (1966).
- [3] P. Möller et al., At. Data. Nucl. Data. Tab. **59**, 185 (1995).

- [4] Yu.Ts. Oganessian and V.K. Utyonkov, Nucl. Phys. A **944**, 62 (2015)
- [5] S. Hofmann et al., Eur. Phys. J. A **32**, 251 (2007).
- [6] L. Stavsetra et al., Phys. Rev. Lett. **103**, 132502 (2009).
- [7] R. Eichler et al., Radiochim. Acta **98**, 133 (2010).
- [8] Ch.E. Düllmann et al., Phys. Rev. Lett. **104**, 252701 (2010).
- [9] P.A. Ellison et al., Phys. Rev. Lett. **105**, 182701 (2010).
- [10] J.M. Gates et al., Phys. Rev. C **83**, 054618 (2011).
- [11] S. Hofmann et al., Eur. Phys. J. A **48**, 62 (2012).
- [12] A. Yakushev et al., Inorg. Chem. **53**, 1624 (2014).
- [13] D. Rudolph et al., Phys. Rev. Lett. **111**, 112502 (2013).
- [14] J. Khuyagbaatar et al., Phys. Rev. Lett. **112**, 172501 (2014).
- [15] D. Kaji et al., J. Phys. Soc. Jpn. **86**, 034201 (2017).
- [16] L. Öhrström and J. Reedijk, Pure and Applied Chemistry **88**, 1225 (2016).
- [17] S. Hofmann et al., GSI Scientific Report-2007, 131 (2008).
- [18] Yu.Ts. Oganessian et al., Phys. Rev. C **79**, 024603 (2009).
- [19] S. Hofmann et al., GSI Scientific Report-2011, 205 (2012).
- [20] Ch.E. Düllmann et al., to be published.
- [21] M.G. Itkis and A. Ya. Rusanov, Phys. Part. Nuclei **29**, 160 (1998).
- [22] C. Simenel et al., Phys. Lett. B **710**, 607 (2012).
- [23] J. Khuyagbaatar et al., GSI Scientific Report-2012, 131 (2013).
- [24] K. Nishio et al., Phys. Rev. C **82**, 024611 (2010).
- [25] J. Khuyagbaatar et al., Phys. Rev. C **91**, 054608 (2015).
- [26] M.G. Itkis et al., Nucl. Phys. A **787**, 150 (2007).
- [27] W.J. Swiatecki, Phys. Scr. **24**, 113 (1981).
- [28] <http://nr.v.jinr.ru/nrv/>
- [29] <http://www.nndc.bnl.gov/>
- [30] K.E. Gregorich et al., Lawrence Berkeley National Laboratory, Berkeley, CA, USA, LBNL-Report 63617 (2007)
- [31] S. Hofmann, Russ. Chem. Rev. **78**, 1123 (2009).
- [32] J. Khuyagbaatar, unpublished data for 3n cross section of the $^{48}\text{Ca}+^{197}\text{Au}$.
- [33] D.J. Hinde et al., Phys. Rev. Lett. **74**, 1295 (1995).
- [34] K. Nishio et al., Phys. Rev. C **77**, 064607 (2008).
- [35] R. Vandenbosch and J. R. Huizenga, Nuclear Fission, Academic, New York, (1973).
- [36] R. Yanez et al., Phys. Rev. Lett. **112**, 152702 (2014).
- [37] P. Möller et al., Phys. Rev. C **79**, 064304 (2009).
- [38] A.C. Berriman et al., Nature (London) **413**, 144 (2001).
- [39] Yu.Ts. Oganessian, J. Phys. G **34**, R165 (2007).
- [40] A. Staszczak et al., Phys. Rev. C, **87**, 024320 (2013).
- [41] A. Mamdouh et al., Nucl. Phys. A **679**, 337 (2001).
- [42] A. Baran et al., Nucl. Phys. A, **944** 442 (2015).
- [43] J. Khuyagbaatar et al., Phys. Rev. Lett. **115**, 242502 (2015).
- [44] A. Mistry, private communication.
- [45] D.A. Mayorov et al., Phys. Rev. C **92**, 054601 (2015).